**MICROSTRUCTURAL ANALYSIS OF A SOIL GRAIN RETURNED FROM ASTEROID ITOKAWA.**

T. J. Zega[1], M. S. Thompson[2], J. Y. Howe[3], [1]Lunar and Planetary Laboratory, Department of Planetary Sciences, University of Arizona, 1629 E. University Blvd, Tucson, AZ, 85721, [2]NASA Johnson Space Center, Mail Code XI3, 2101 E NASA Parkway, Houston, TX, 77058, [3]Hitachi High-Technologies America Inc., 22610 Gateway Center Drive, Suite 100 Clarksburg, MD 20871.

**Introduction:** The Hayabusa spacecraft was launched on May 9, 2003 to test sample-return from a near-Earth asteroid. It rendezvoused with asteroid 25413 Itokawa in September 2005 and returned to Earth on June 13, 2010 carrying in excess of 1,500 particles with sizes up to 180 μm. Preliminary examination by the science team included a host of measurements. X-ray diffraction, transmission electron microscopy, and scanning electron microscope analyses showed that the Itokawa dust particles have a mineralogy identical to that of thermally metamorphosed LL chondrites [1-4]. These and other measurements established the link between ordinary chondrites and S-type asteroids [1-4].

Many of the particles contain evidence of surface modification due to space weathering, e.g., [5]. For example, Fe and Fe-S nanoparticles occur within a surface layer on several silicate minerals including olivine, low-Ca pyroxene, plagioclase, and in glassy material. In a later study [6], our group identified partially and completely amorphous rims, vesiculated rim textures, npFe, amorphous surface islands, and multilayered rim structures with chemical and structural heterogeneity. Here we report new results from measurements of an Itokawa particle as part of a longer-term study aimed at understanding asteroidal surface processes and space weathering.

**Sample and Methods:** We were allocated sample RA-QD02-0248 from the NASA JSC Hayabusa Curation Laboratory. Scanning electron microscope images acquired during curation show that the sample measured approximately 148 μm across; Energy-dispersive X-ray spectra (EDS) from three different points within the sample suggest several different mineral phases occur, including olivine, plagioclase, high-Ca pyroxene and troilite [7].

We embedded the grain in a low-viscosity epoxy and prepared it for transmission electron microscope (TEM) analysis using a hybrid ultramicrotome/focused-ion-beam (FIB) approach developed by [8]. The method involved mechanical slicing of the first several hundred nm of the grain with a diamond knife, depositing the slices onto lacey-C TEM grids.

After ultramicrotomy, the epoxy bullet was placed into the FIB for secondary and backscattered-electron imaging and EDS analysis. Based upon the imaging results and X-ray spectroscopy, we chose five different areas of the sample for FIB cross sectioning and extraction. Four of the five FIB sections were prepared using the FEI Helios Nanolab 660 FIB-SEM located at the Lunar and Planetary Laboratory (LPL), University of Arizona, equipped with an EDAX EDS system and electron backscatter detector. The fifth FIB section was prepared at Hitachi High-Technologies Co. in Naka, Japan.

All sections were analyzed for their detailed structure and composition using TEM techniques. Several TEMs were used for this work: The 300 keV Hitachi HF3300 at the University of Toronto equipped with bright-field (BF), dark-field (DF), and secondary-electron (SE) detectors as well as a Bruker Si-drift EDS system; the 200 keV aberration-corrected Hitachi HF5000 currently being installed at LPL, University of Arizona, and equipped with BF, DF, and SE detctors as well as Oxford dual-side-entry Si-drift EDS detectors giving a large (2.0 sr) solid angle; and the 200 keV aberration-corrected Hitachi HF5000 TEM at Hitachi High Technologies, Naka, Japan equipped similarly to the HF5000 at LPL.

**Results:** Reflected-light optical images show that ultramicrotome slicing was successful in exposing a flat face of sample RA-QD02-0248, effectively polishing its surface. The as-sliced particle measures approximately 100 μm × 50 μm. EDS mapping in the FIB shows that olivine is the most abundant component (by area) of the sample, followed by pyroxene, and plagioclase (Fig. 1). No sulfide was identified.

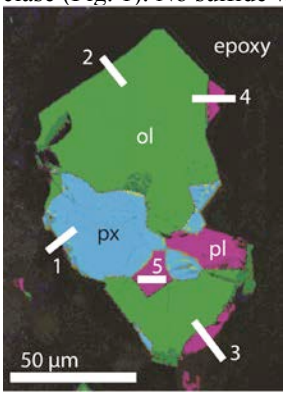


**Figure 1:** EDS phase map showing the surface of the grain after microtoming. Mineral phases present in the grain include plagioclase (pink), olivine (green), and pyroxene (blue). White lines (1-5) indicate locations from which FIB sections were extracted.

*Section 1* transects the pyroxene region, as shown in the surface phase map on the left side of the grain (Fig. 1). However, TEM-EDS mapping of the section reveals a Ca-Al-Si-O domain on the left and an Fe-Mg domain on the right. BF-TEM imaging and selected-

area electron-diffraction (SAED) patterns show that this slice is polycrystalline and contains high-Ca pyroxene/pigeonite (left) and forsterite (right).

*Section 2* transects the olivine region, as indicated in the surface phase map (Fig. 1). BF-TEM imaging and SAED patterns show that the section contains a single crystal of olivine. EDS mapping shows that the olivine contains Fe, Mg with minor Ca, Mn, and Ni. BF images reveal fine-scale lamellae along the base of the section. The olivine contains a crystalline rim measuring ~50 nm thick with elemental ratios identical to the bulk crystal.

*Section 3* transects the plagioclase and olivine domains, as revealed in the surface phase map (Fig. 1). BF imaging and SAED patterns reveal two crystals of forsterite and anorthite. BF and DF imaging also show numerous inclusions with varied sizes (tens to approximately 200 nm). EDS maps show that the inclusions are composed of Na and Cl (Fig. 2). SE images reveal that some of these inclusions occur on the surface of the section but some may also be within the thickness of the slice. DF images also show fine-scale (<100 nm) lamellae occur along the edge of the anorthite and which extend at an oblique angle to the interface with the olivine. EDS mapping reveal that the lamellae are depleted in Na and enriched in K.

*Section 4* also transects the plagioclase and olivine domains but in a different location than Section 3 (see Fig. 1). SAED reveals a single crystal of olivine. The plagioclase contains fine-scale lamellae as shown in the BF image. Similar to Section 3, the lamellae are depleted in Na and enriched in K.

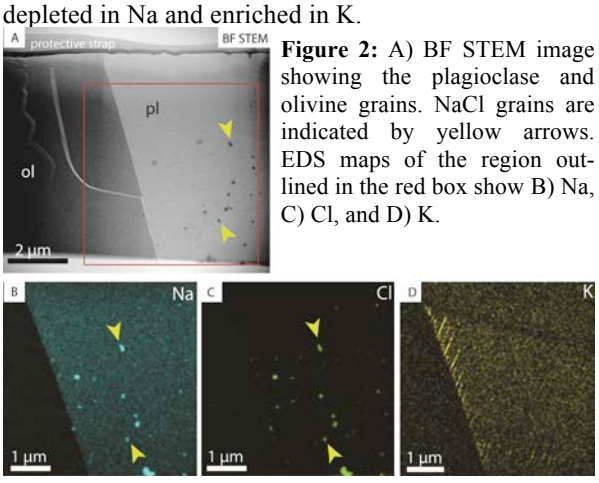


**Figure 2:** A) BF STEM image showing the plagioclase and olivine grains. NaCl grains are indicated by yellow arrows. EDS maps of the region outlined in the red box show B) Na, C) Cl, and D) K.

*Section 5* transects only the plagioclase domain as shown in the surface map (Fig. 1). BF imaging and SAED show that twin lamellae extend across the width of the entire section. EDS mapping reveals that the lamellae are depleted in K, and one appears to be enriched in Na. We observe a small (100 nm) inclusion particle that appears to be enriched in Cl.

**Discussion:** Previous work suggest that particles in the MUSES-C Regio experienced thermal modification: K-feldspar exsolution from plagioclase was estimated to occur at a peak temperature of 820 ℃ [1]. Similarly, our results from Section 4 indicate exsolution of K-feldspar from the host anorthite, suggesting similar temperature constraints. However, our analyses of Section 5 present conflicting results, with exsolved lamellae enriched in Na, and depleted in K. Possible thermodynamic constraints applicable to this new microstructure will be discussed at the meeting.

The presence of NaCl and KCl crystals associated with samples returned from Itokawa has been reported previously [7]. However, these µm-sized particles were present on the surfaces of analyzed grains and, barring evidence for extra-terrestrial origin, are thought to be the product of contamination in the sample catcher. In contrast, the results presented here demonstrate that at least some of the NaCl and KCl particles appear to be embedded as inclusions *within* the plagioclase grain, and are not surface-correlated. These inclusions are present in two distinct FIB sections which were prepared in different laboratories, both designed to limit the section's exposure to air and thus potential contamination. Although additional characterization of this and other sections is required to verify NaCl inclusions, the data indicate there is a possibility that these grains are not alteration products but may indeed be native to the sample. The presence of NaCl and KCl is not novel in ordinary chondrite materials, having been identified in H-chondrite breccias Zag and Monahans [9-13]. Though seemingly rare, if the NaCl and KCl in LL samples reported here is confirmed as being extra-terrestrial in origin, it may suggest that these minerals are much more common on ordinary chondrite bodies than previously thought.

**References:** [1] Nakamura, T. et al. (2011) *Science*, *333,* 1113-1116. [2] Tsuchiyama A. et al. (2011) *Science, 333,* 1125-1128. [3] Yurimoto, H. et al. (2011) *Science, 333,* 1116-1119. [4] Nagao K. et al. (2011) *Science, 333,* 1128-1131. [5] Noguchi T. et al. (2011). *Science 333*, 1121-1125. [6] Thompson M. S. et al. (2014) *Earth. Planet. Space., 66,* 1-10. [7] Hayabusa Collection Information, *NASA Curation*, https://curator.jsc.nasa.gov/hayabusa/samples/hayabusa-spectra.cfm?sample=RA-QD02-0248. [8] Berger. E. L. and Keller L P. (2015) *Microscopy Today*, *23,* 18-23. [9] Noguchi, T. et al. (2014) *Meteorit. Planet. Sci., 49*, 1305–1314. [10] Zolensky M. E. et al. (1999) *Science, 285:*1377–1379. [11] Whitby J. A. et al. (2000) *Science, 208*:1819–1821. [12] Rubin A. E. et al. (2002). *Meteorit. Planet. Sci. 37,* 125–141. [13] Bridges J. C. et al. (2004) *Meteorit. Planet. Sci. 39,* 657–666.